Electron Supporting Information

Rare-earth metal mediated PhC≡N insertion into *N*,*N*-bis(trimethylsilyl)naphthalene-1,8-diamido dianion – a synthetic approach to complexes coordinated by *ansa*-bridged amido-amidinato ligand. Synthesis, structures and catalytic activity in ring-opening polymerization of *rac*-lactide

Dmitry M. Lyubov,[a] Anton V. Cherkasov,[a] Georgy K. Fukin,[a] Konstantin A. Lyssenko,[b] Elena A. Rychagova,[a] Sergey Yu. Ketkov,[a] Alexander A. Trifonov[a,b,*]

[a]Institute of Organometallic Chemistry of Russian Academy of Sciences, Tropinina 49, GSP-445, 630950, Nizhny Novgorod (Russia) Fax: 007831 4627497; Tel: 007 831 4623532; E-mail: trif@iomc.ras.ru
[b]Institute of Organoelement compounds of Russian Academy of Sciences, Vavilova str. 28, 119334, Moscow, Russia.

Contents

Fig 1. ^{1}H NMR spectrum of 1,8-$C_{10}H_6[N(SiMe_3)Li(OEt_2)]_2$ (**1**$^{\mathbf{Et2O}}$).

Fig 2. $^{13}C\{^{1}H\}$ NMR spectrum of 1,8-$C_{10}H_6[N(SiMe_3)Li(OEt_2)]_2$ (**1**$^{\mathbf{Et2O}}$).

Fig 3. $^{7}Li\{^{1}H\}$ NMR spectrum of 1,8-$C_{10}H_6[N(SiMe_3)Li(OEt_2)]_2$ (**1**$^{\mathbf{Et2O}}$).

Fig 4. ^{1}H NMR spectrum of 1,8-$C_{10}H_6[N(SiMe_3)Li(TMEDA)]_2$ (**1**$^{\mathbf{TMEDA}}$).

Fig 5. $^{13}C\{^{1}H\}$ NMR spectrum of 1,8-$C_{10}H_6[N(SiMe_3)Li(TMEDA)]_2$ (**1**$^{\mathbf{TMEDA}}$).

Fig 6. $^{7}Li\{^{1}H\}$ NMR spectrum of 1,8-$C_{10}H_6[N(SiMe_3)Li(TMEDA)]_2$ (**1**$^{\mathbf{TMEDA}}$).

Fig 7. ^{1}H NMR spectrum of 1,8-$C_{10}H_6[N(SiMe_3)Li(N{\equiv}CPh)(OEt_2)][N(SiMe_3)Li(OEt_2)]$ (**2**$^{\mathbf{Et2O}}$).

Fig 8. $^{13}C\{^{1}H\}$ NMR spectrum of 1,8-$C_{10}H_6[N(SiMe_3)Li(N{\equiv}CPh)(OEt_2)][N(SiMe_3)Li(OEt_2)]$ (**2**$^{\mathbf{Et2O}}$).

Fig 9. $^{7}Li\{^{1}H\}$ NMR spectrum of 1,8-$C_{10}H_6[N(SiMe_3)Li(N{\equiv}CPh)(OEt_2)][N(SiMe_3)Li(OEt_2)]$ (**2**$^{\mathbf{Et2O}}$).

Fig 10. ^{1}H NMR spectrum of 1,8-$C_{10}H_6[N(SiMe_3)Li(N{\equiv}CPh)][N(SiMe_3)Li(TMEDA)]$ (**2**$^{\mathbf{TMEDA}}$).

Fig 11. $^{13}C\{^{1}H\}$ NMR spectrum of 1,8-$C_{10}H_6[N(SiMe_3)Li(N{\equiv}CPh)][N(SiMe_3)Li(TMEDA)]$ (**2**$^{\mathbf{TMEDA}}$).

Fig 12. $^{7}Li\{^{1}H\}$ NMR spectrum of 1,8-$C_{10}H_6[N(SiMe_3)Li(N{\equiv}CPh)][N(SiMe_3)Li(TMEDA)]$ (**2**$^{\mathbf{TMEDA}}$).

Fig. 13. ^{1}H NMR spectrum of [{1,8-$C_{10}H_6[NSiMe_3][NC(Ph)NSiMe_3]$}{1,8-$C_{10}H_6[N(H)SiMe_3][NC(Ph)NSiMe_3]$}YCl][$Li(THF)_4$] (**3Y**).

Fig. 14. $^{13}C\{^{1}H\}$ NMR spectrum of [{1,8-$C_{10}H_6[NSiMe_3][NC(Ph)NSiMe_3]$}{1,8-$C_{10}H_6[N(H)SiMe_3][NC(Ph)NSiMe_3]$}YCl][$Li(THF)_4$] (**3Y**).

Fig. 15. $^{7}Li\{^{1}H\}$ NMR spectrum of $[\{1,8\text{-}C_{10}H_6[NSiMe_3][NC(Ph)NSiMe_3]\}\{1,8\text{-}C_{10}H_6[N(H)SiMe_3][NC(Ph)NSiMe_3]\}YCl][Li(THF)_4]$ (**3Y**).

Fig. 16. ^{1}H NMR spectrum of $\{1,8\text{-}C_{10}H_6[NSiMe_3][NC(Ph)NSiMe_3)]\}YCl(TMEDA)$ (**4**).

Fig. 17. $^{13}C\{^{1}H\}$ NMR spectrum of $\{1,8\text{-}C_{10}H_6[NSiMe_3][NC(Ph)NSiMe_3)]\}YCl(TMEDA)$(**4**).

Fig. 18. ^{1}H NMR spectrum of $[\{1,8\text{-}C_{10}H_6[NSiMe_3][NC(Ph)NSiMe_3]\}\{1,8\text{-}C_{10}H_6[N(H)SiMe_3][NC(Ph)NSiMe_3]\}YOtBu][Li(THF)_4]$ (**7**).

Fig. 19. $^{13}C\{^{1}H\}$ NMR spectrum of $[\{1,8\text{-}C_{10}H_6[NSiMe_3][NC(Ph)NSiMe_3]\}\{1,8\text{-}C_{10}H_6[N(H)SiMe_3][NC(Ph)NSiMe_3]\}YOtBu][Li(THF)_4]$ (**7**).

Fig. 20. $^{7}Li\{^{1}H\}$ NMR spectrum of $[\{1,8\text{-}C_{10}H_6[NSiMe_3][NC(Ph)NSiMe_3]\}\{1,8\text{-}C_{10}H_6[N(H)SiMe_3][NC(Ph)NSiMe_3]\}YOtBu][Li(THF)_4]$ (**7**).

Fig. 21. ^{1}H NMR spectrum of $\{1,8\text{-}C_{10}H_6[NSiMe_3][NC(Ph)NSiMe_3]\}YOtBu(TMEDA)$ (**8**).

Fig. 22. $^{13}C\{^{1}H\}$ NMR spectrum of $\{1,8\text{-}C_{10}H_6[NSiMe_3][NC(Ph)NSiMe_3]\}YOtBu(TMEDA)$ (**8**).

Fig. 23. Isosurfaces (isovalue 0.02) of the frontier molecular orbitals in complexes **2'** and **4'**.

Table S1. Crystal data and structure refinement for complexes $\mathbf{2^{Et2O}}$, $\mathbf{2^{TMEDA}}$, **3Y**, **3Sm**, **4**, **7**, **8**.

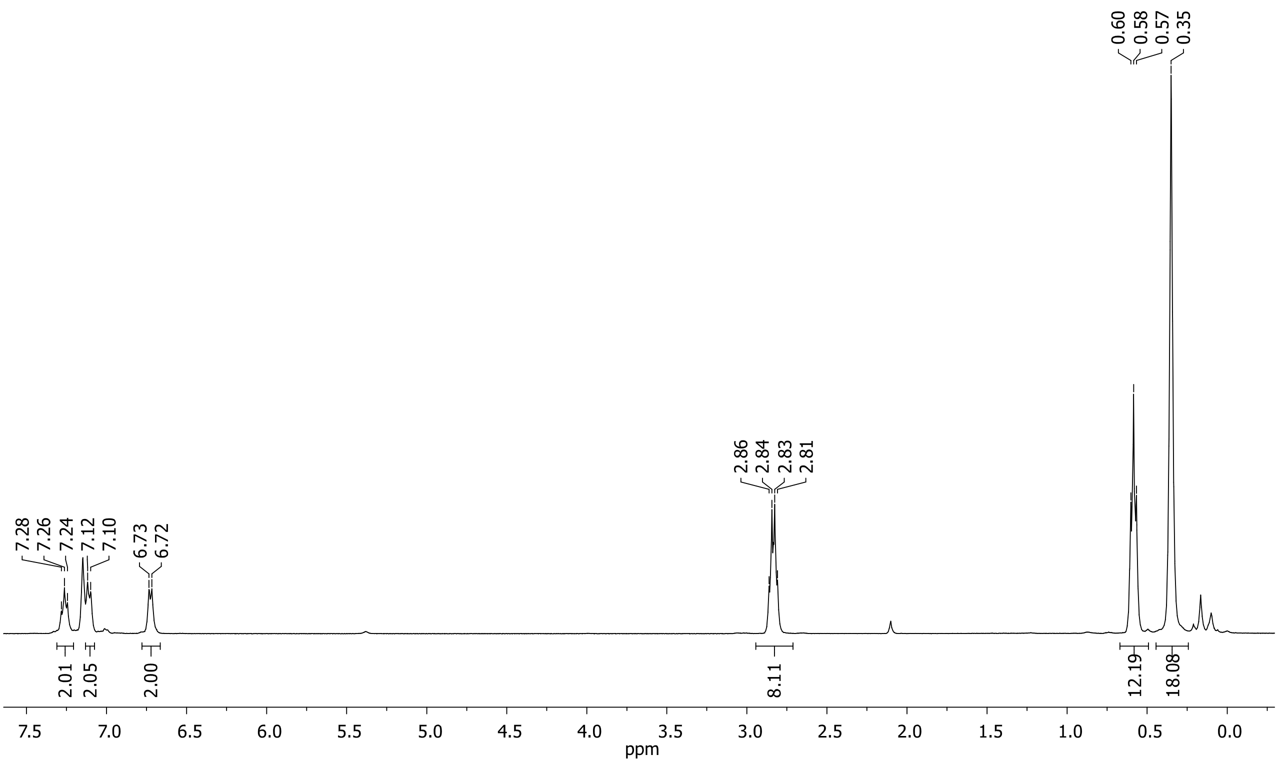

Fig 1. ^{1}H NMR spectrum of 1,8-$C_{10}H_6[N(SiMe_3)Li(OEt_2)]_2$ (**1^{Et2O}**) (400 MHz, C_6D_6, 293 K).

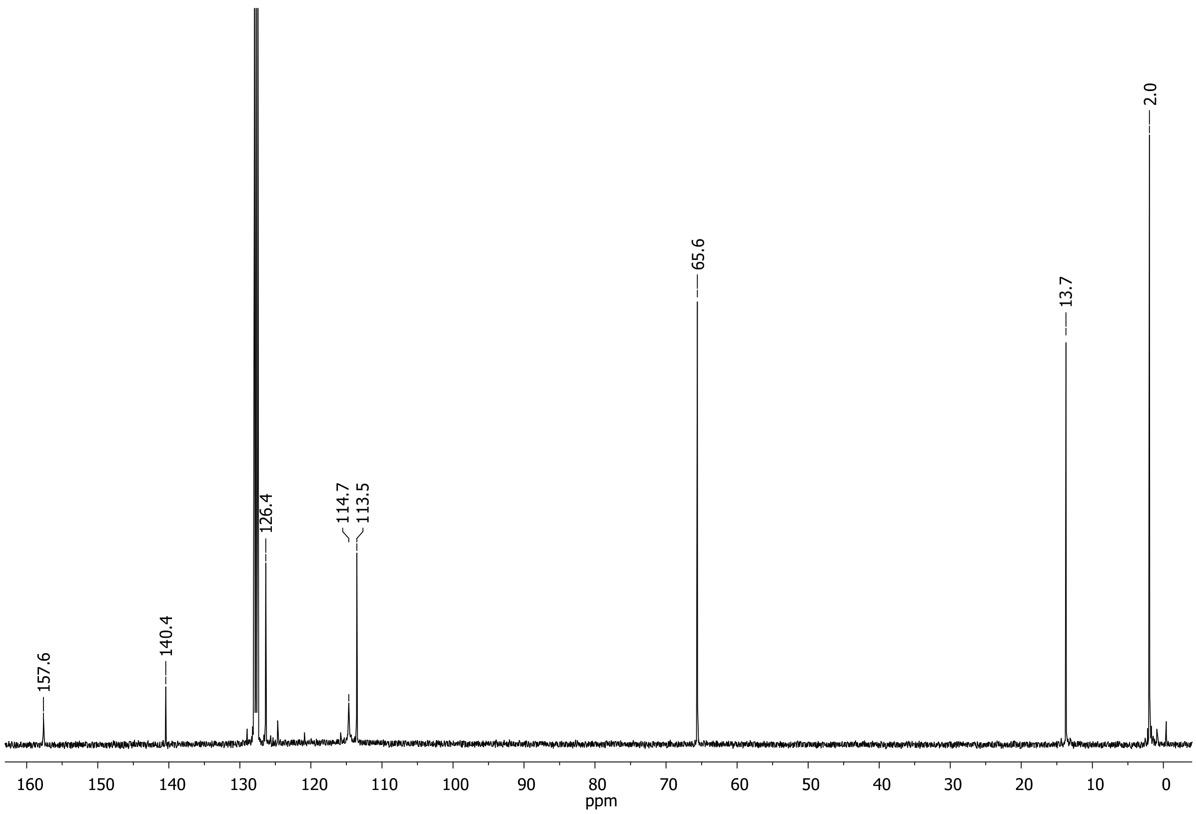

Fig 2. $^{13}C\{^{1}H\}$ NMR spectrum of 1,8-$C_{10}H_6[N(SiMe_3)Li(OEt_2)]_2$ (**1^{Et2O}**) (100 MHz, C_6D_6, 293 K).

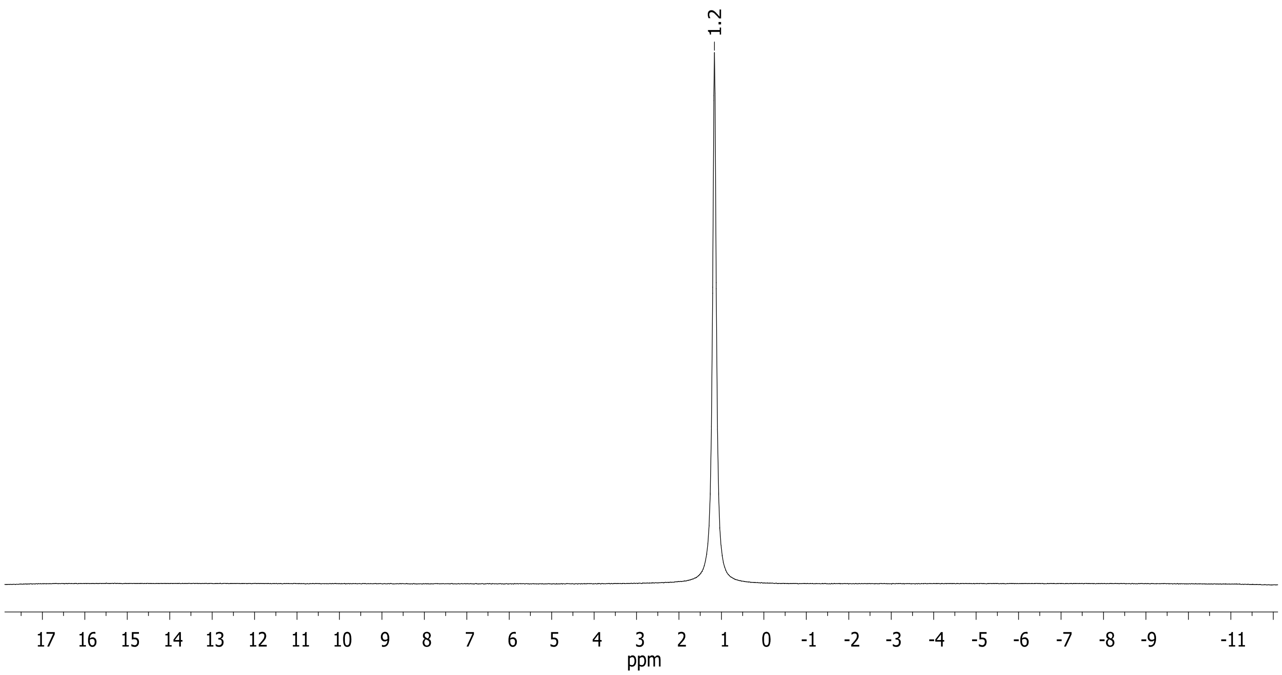

Fig 3. $^{7}Li\{^{1}H\}$ NMR spectrum of 1,8-$C_{10}H_6[N(SiMe_3)Li(OEt_2)]_2$ (**1^{Et2O}**) (155.5 MHz, C_6D_6, 293K).

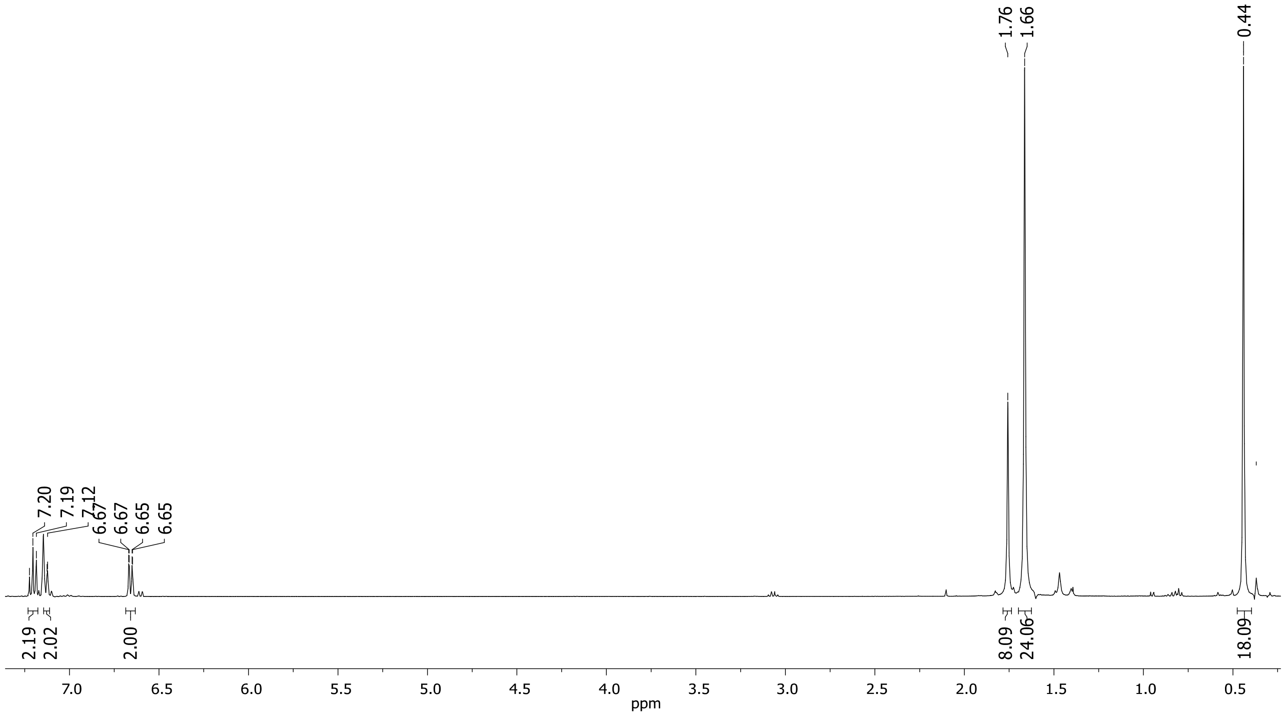

Fig 4. ^{1}H NMR spectrum of 1,8-$C_{10}H_6[N(SiMe_3)Li(TMEDA)]_2$(**1^{TMEDA}**) (400 MHz, C_6D_6, 293 K).

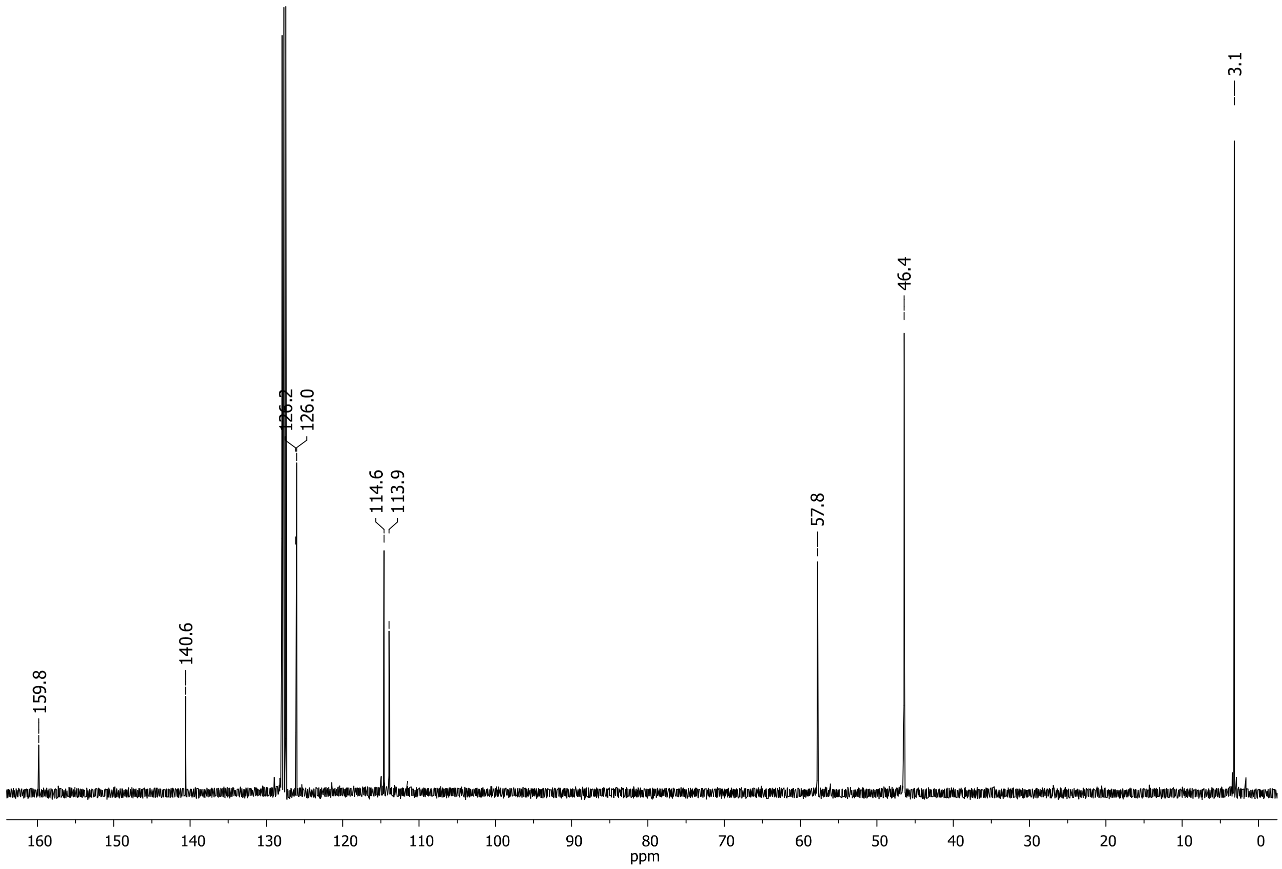

Fig 5. $^{13}C\{^{1}H\}$ NMR spectrum of 1,8-$C_{10}H_6[N(SiMe_3)Li(TMEDA)]_2$ (**1^{TMEDA}**) (100 MHz, C_6D_6, 293 K).

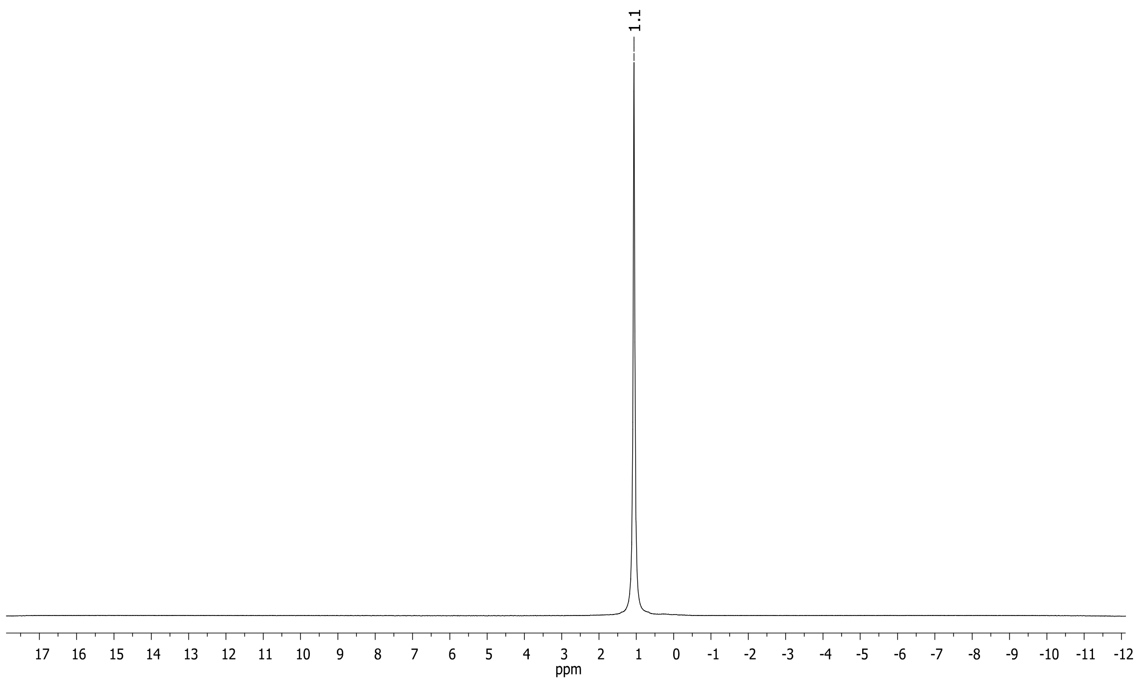

Fig 6. $^{7}Li\{^{1}H\}$ NMR spectrum of 1,8-$C_{10}H_6[N(SiMe_3)Li(TMEDA)]_2$ (**1^{TMEDA}**) (155.5 MHz, C_6D_6, 293 K).

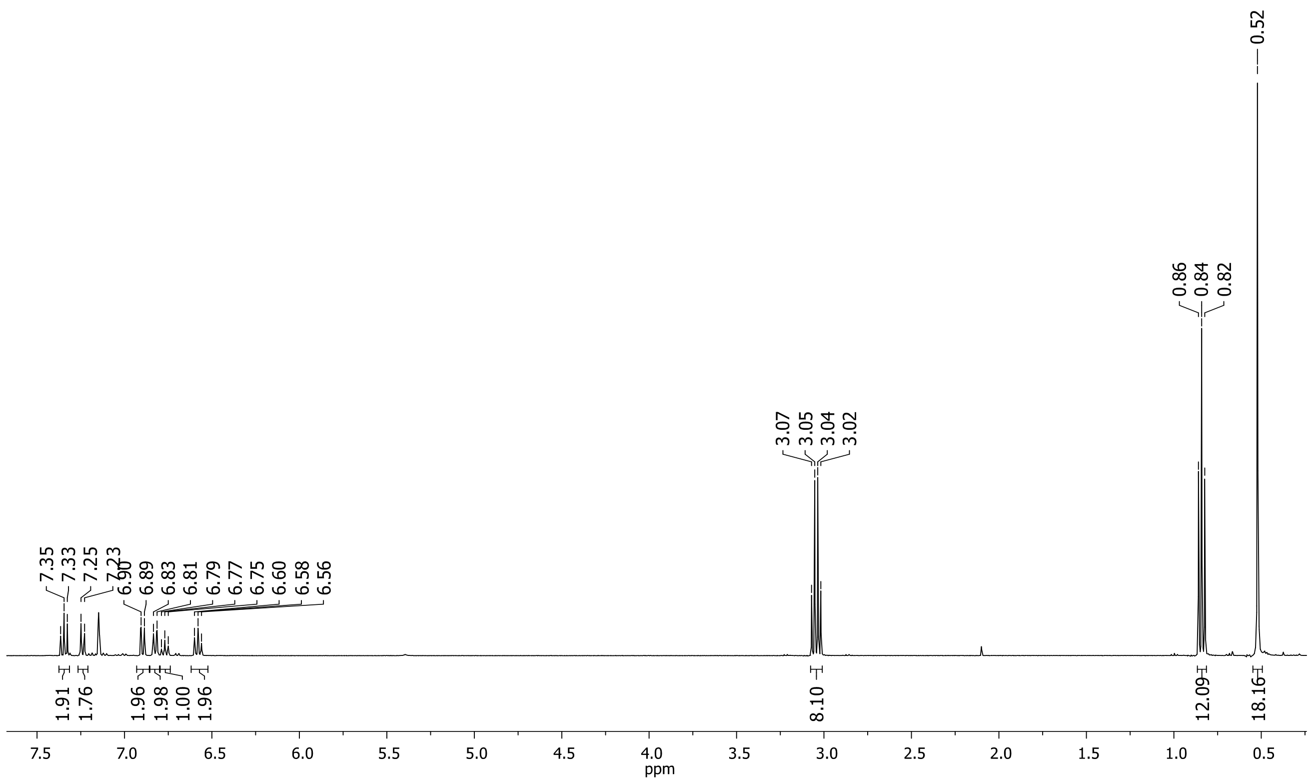

Fig 7. ^{1}H NMR spectrum of 1,8-$C_{10}H_6$[N($SiMe_3$)Li(N≡CPh)(OEt_2)][N($SiMe_3$)Li(OEt_2)] (**2**$^{\mathbf{Et2O}}$) (400 MHz, C_6D_6, 293 K).

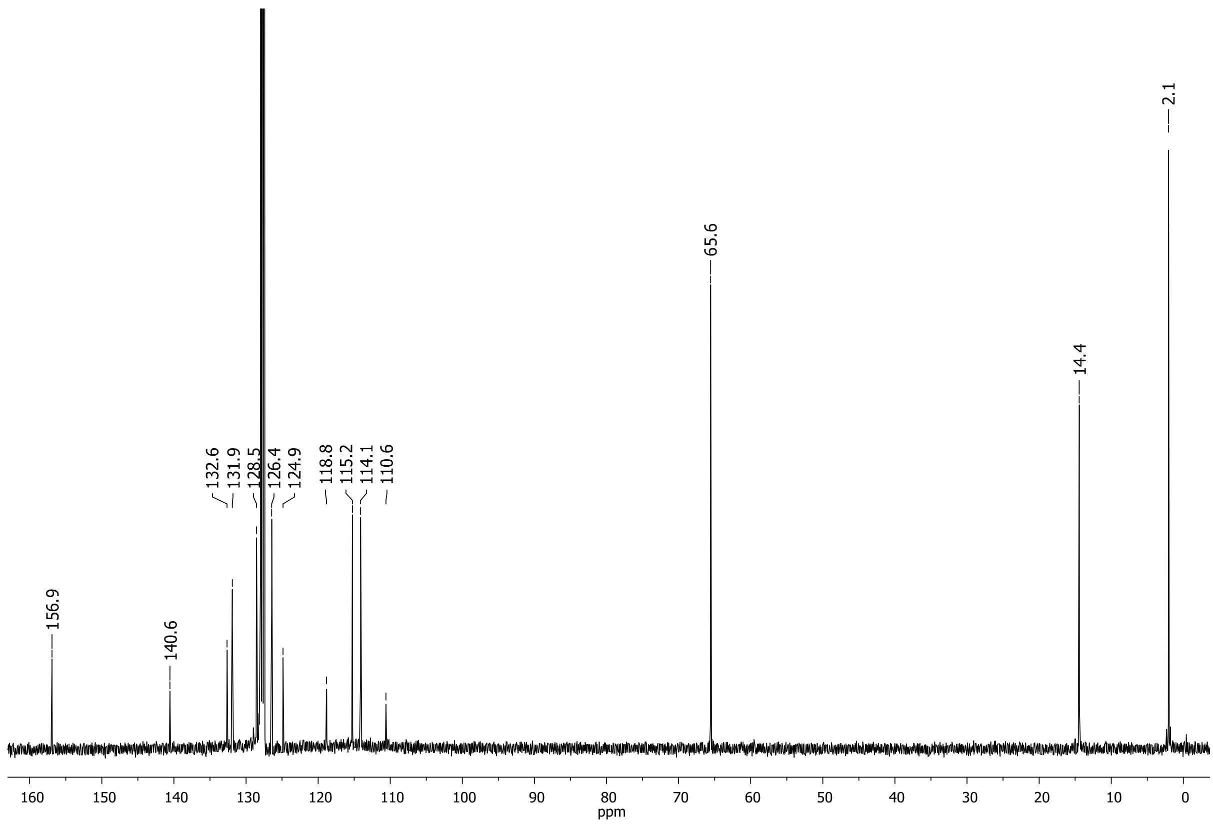

Fig 8. $^{13}C\{^1H\}$ NMR spectrum of 1,8-$C_{10}H_6$[N($SiMe_3$)Li(N≡CPh)(OEt_2)][N($SiMe_3$)Li(OEt_2)] (**2**$^{\mathbf{Et2O}}$) (100 MHz, C_6D_6, 293 K).

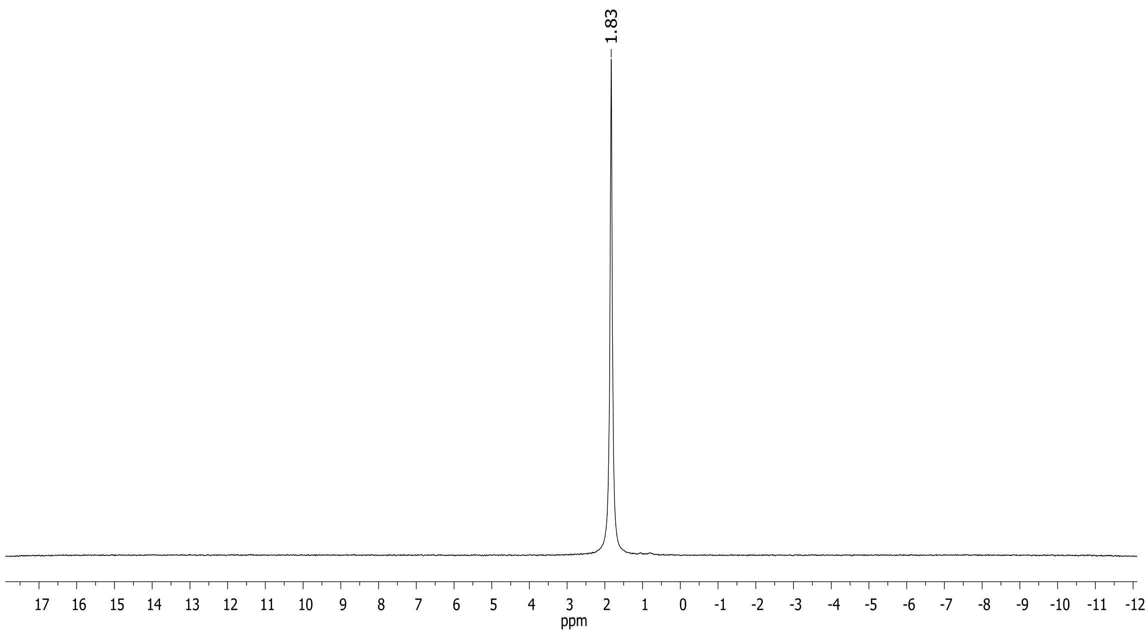

Fig 9. $^{7}Li\{^{1}H\}$ NMR spectrum of 1,8-$C_{10}H_6$[N($SiMe_3$)Li(N≡CPh)(OEt_2)][N($SiMe_3$)Li(OEt_2)] ($\mathbf{2}^{\mathbf{Et2O}}$) (155.5 MHz, C_6D_6, 293 K).

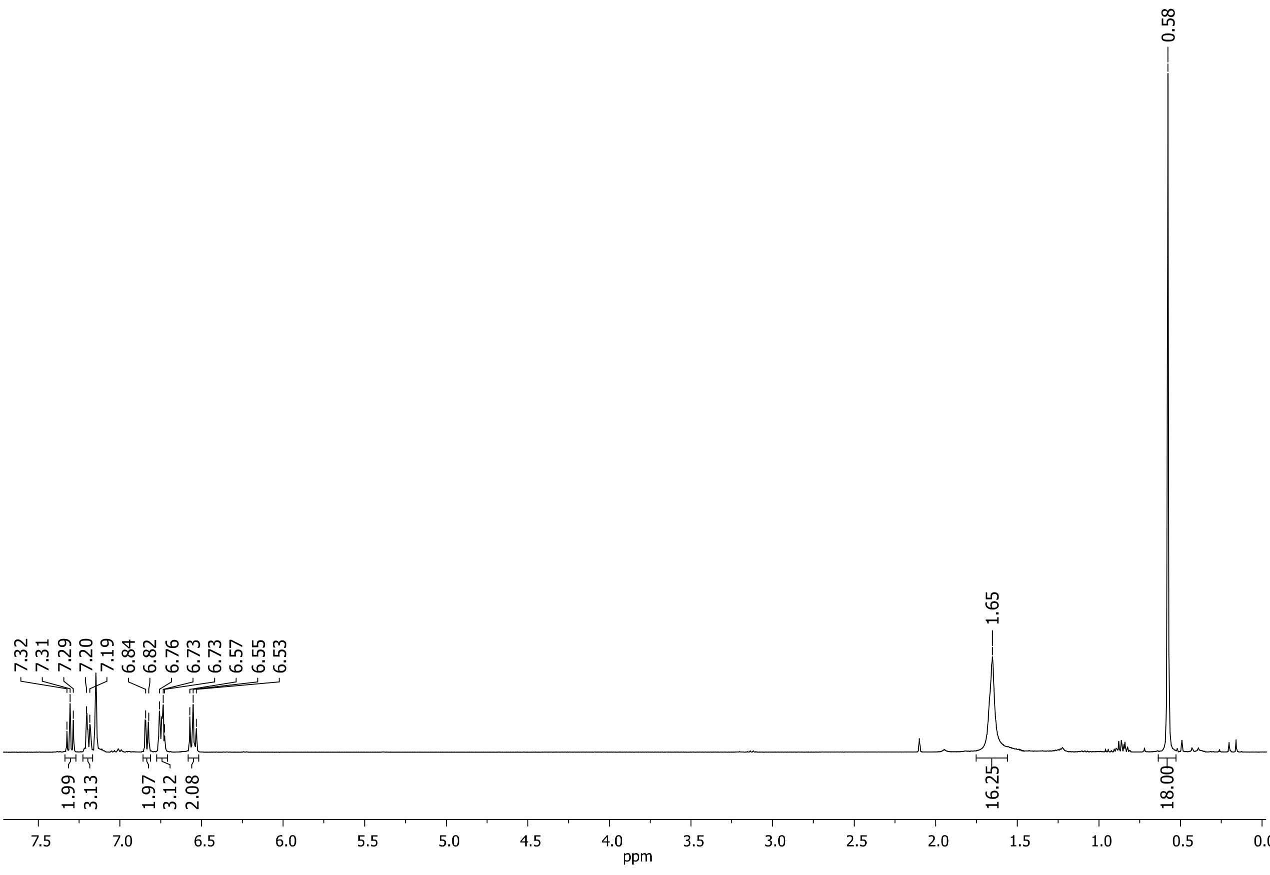

Fig 10. ^{1}H NMR spectrum of 1,8-$C_{10}H_6$[N($SiMe_3$)Li(N≡CPh)][N($SiMe_3$)Li(TMEDA)] ($\mathbf{2}^{\mathbf{TMEDA}}$) (400 MHz, C_6D_6, 293 K).

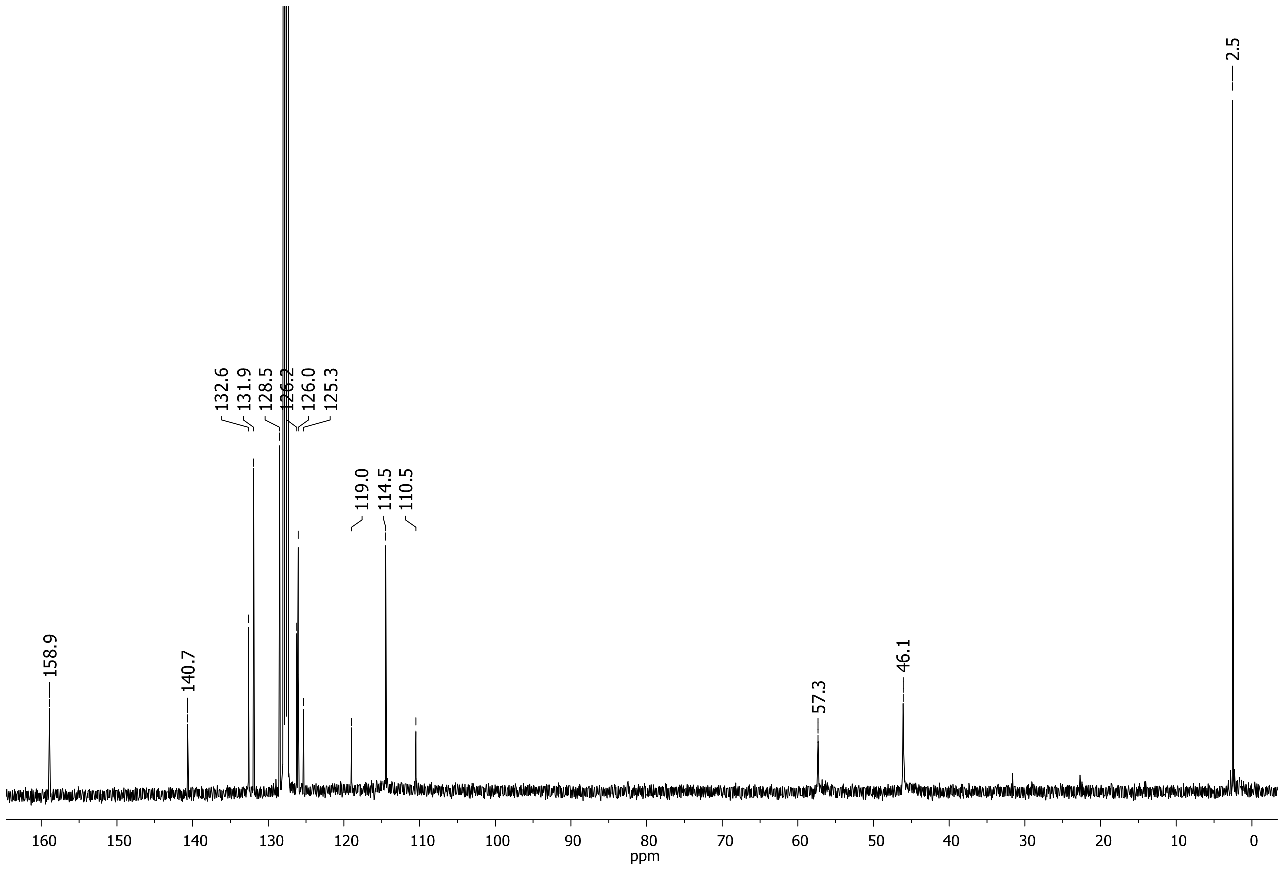

Fig 11. $^{13}C\{^{1}H\}$ NMR spectrum of 1,8-$C_{10}H_6[N(SiMe_3)Li(N{\equiv}CPh)][N(SiMe_3)Li(TMEDA)]$ ($\mathbf{2}^{\mathbf{TMEDA}}$) (100 MHz, C_6D_6, 293 K).

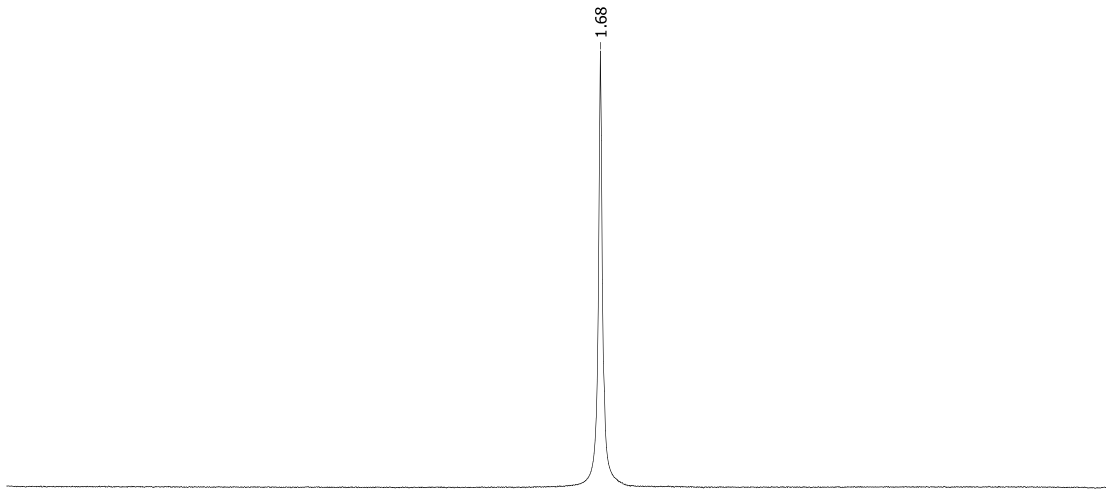

Fig 12. $^{7}Li\{^{1}H\}$ NMR spectrum of 1,8-$C_{10}H_6[N(SiMe_3)Li(N{\equiv}CPh)][N(SiMe_3)Li(TMEDA)]$ ($\mathbf{2}^{\mathbf{TMEDA}}$) (155.5 MHz, C_6D_6, 293 K).

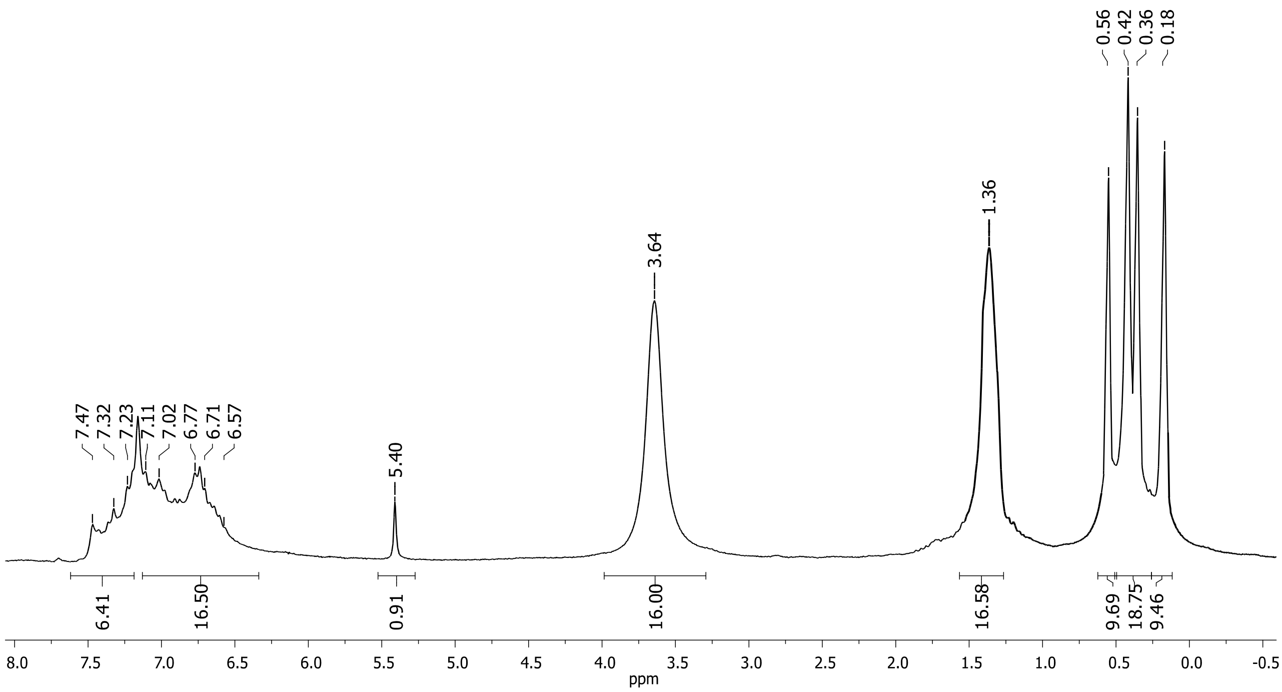

Fig. 13. ^{1}H NMR spectrum of [{1,8-$C_{10}H_6$[$NSiMe_3$][NC(Ph)$NSiMe_3$]}{1,8-$C_{10}H_6$[N(H)$SiMe_3$][NC(Ph)$NSiMe_3$]}YCl][Li$(THF)_4$] (**3Y**) (200 MHz, C_6D_6, 293 K).

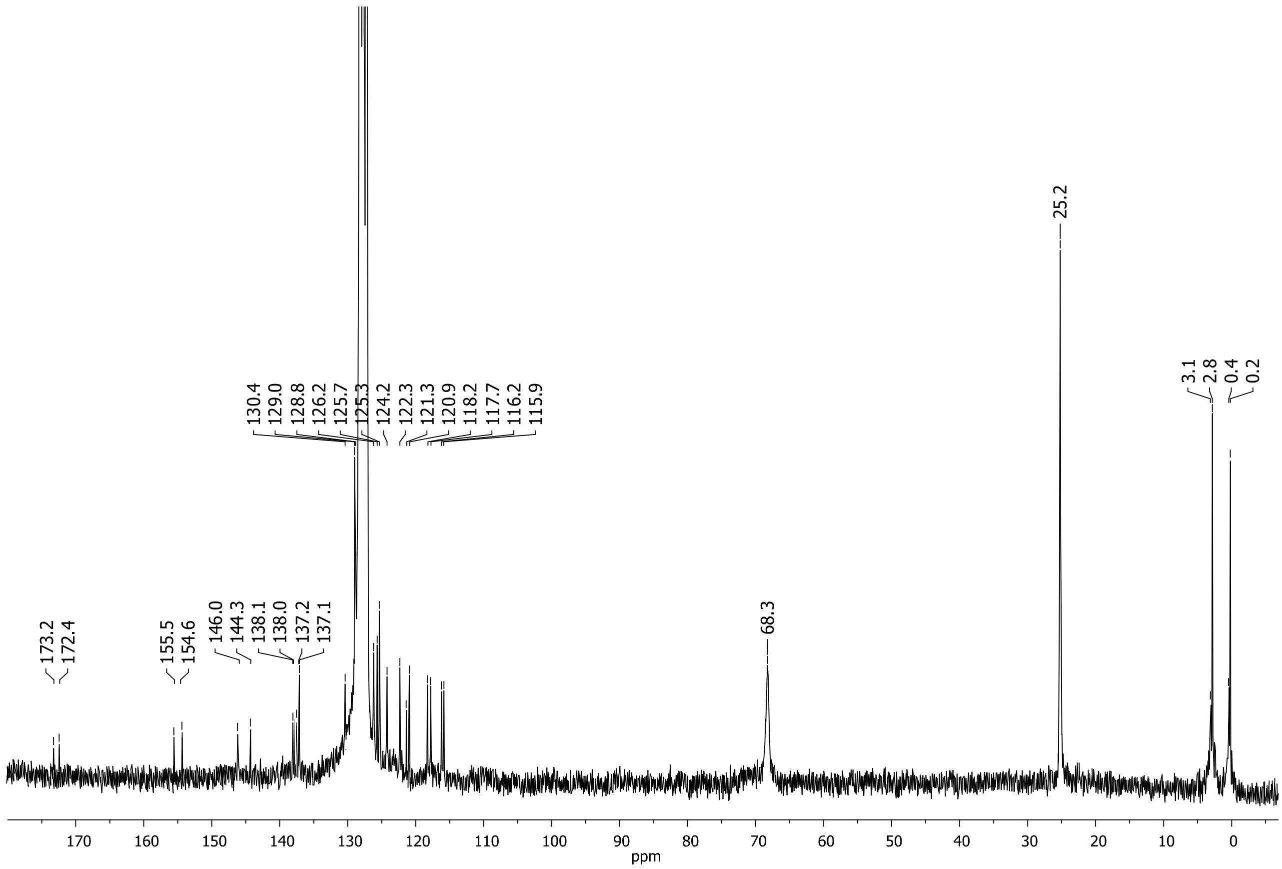

Fig. 14. ^{13}C{^{1}H} NMR spectrum of [{1,8-$C_{10}H_6$[$NSiMe_3$][NC(Ph)$NSiMe_3$]}{1,8-$C_{10}H_6$[N(H)$SiMe_3$][NC(Ph)$NSiMe_3$]}YCl][Li$(THF)_4$] (**3Y**) (50 MHz, C_6D_6, 293 K).

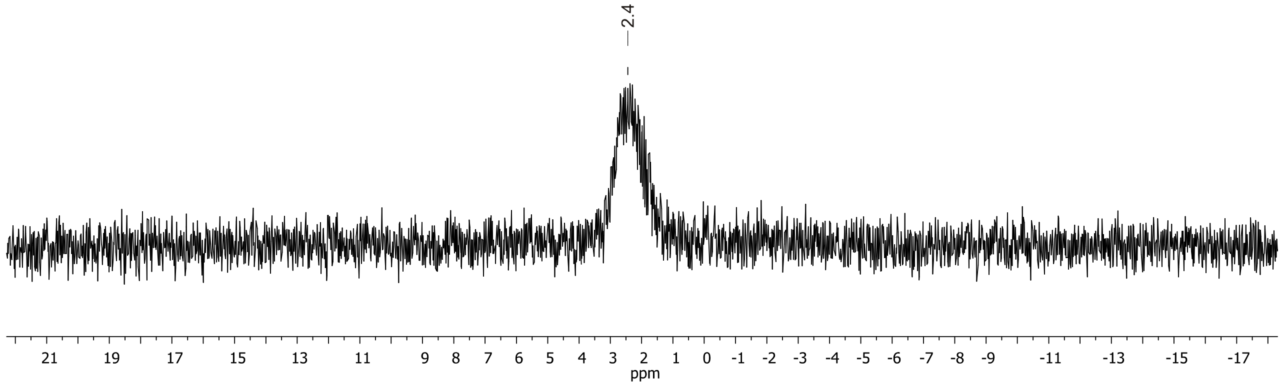

Fig. 15. $^{7}Li\{^{1}H\}$ NMR spectrum of [{1,8-$C_{10}H_6$[$NSiMe_3$][NC(Ph)$NSiMe_3$]}{1,8-$C_{10}H_6$[N(H)$SiMe_3$][NC(Ph)$NSiMe_3$]}YCl][Li$(THF)_4$] (**3Y**) (77.7 MHz, C_6D_6, 293 K).

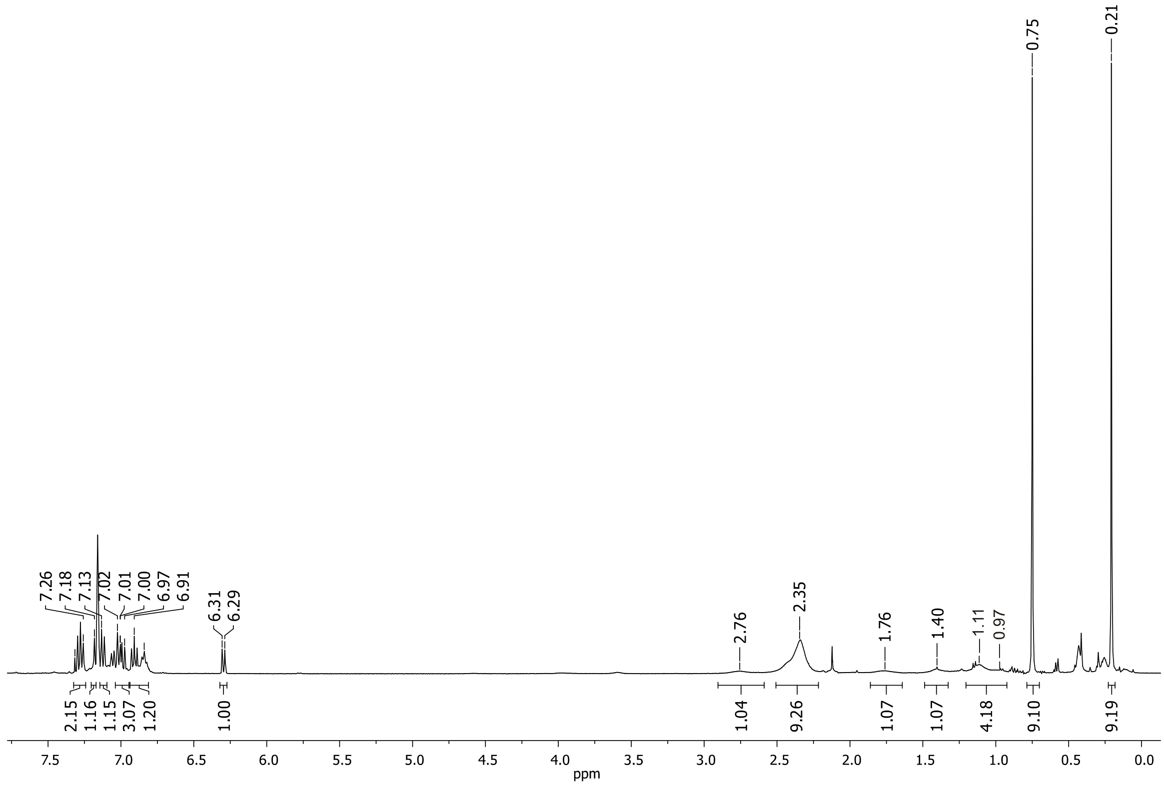

Fig. 16. ^{1}H NMR spectrum of {1,8-$C_{10}H_6$[$NSiMe_3$][NC(Ph)$NSiMe_3$)]}YCl(TMEDA) (**4**) (400 NHz, C_6D_6, 293 K).

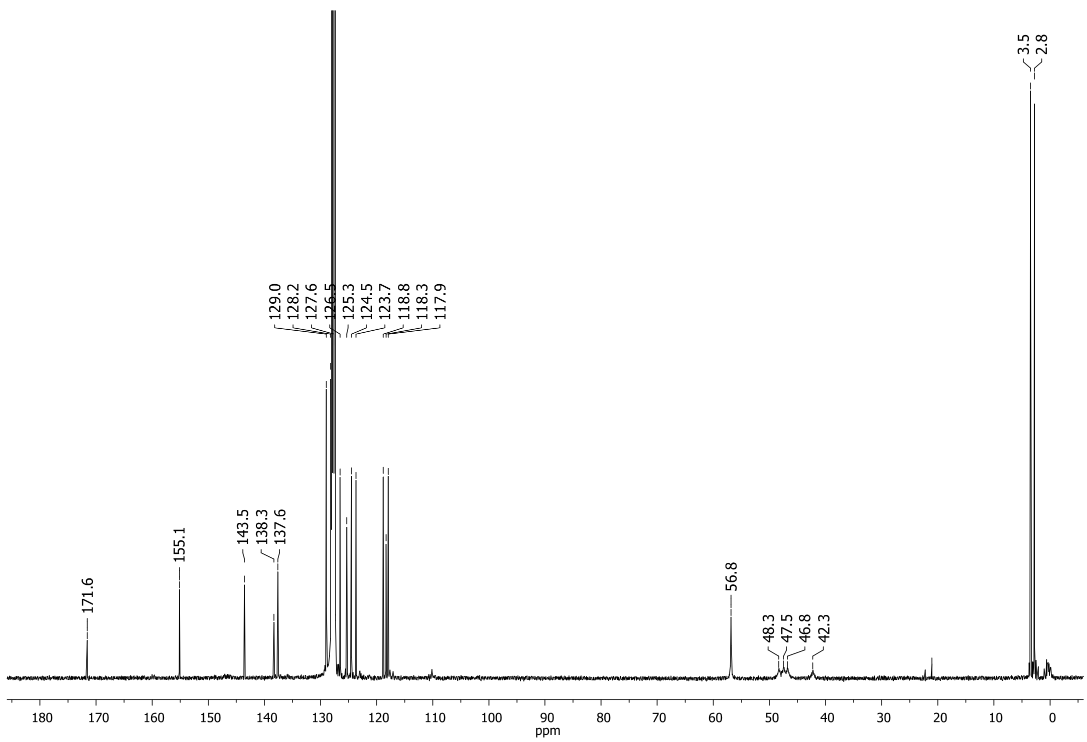

Fig. 17. $^{13}C\{^1H\}$ NMR spectrum of $\{1,8\text{-}C_{10}H_6[NSiMe_3][NC(Ph)NSiMe_3)]\}YCl(TMEDA)$ (**4**) (100 MHz, C_6D_6, 293 K).

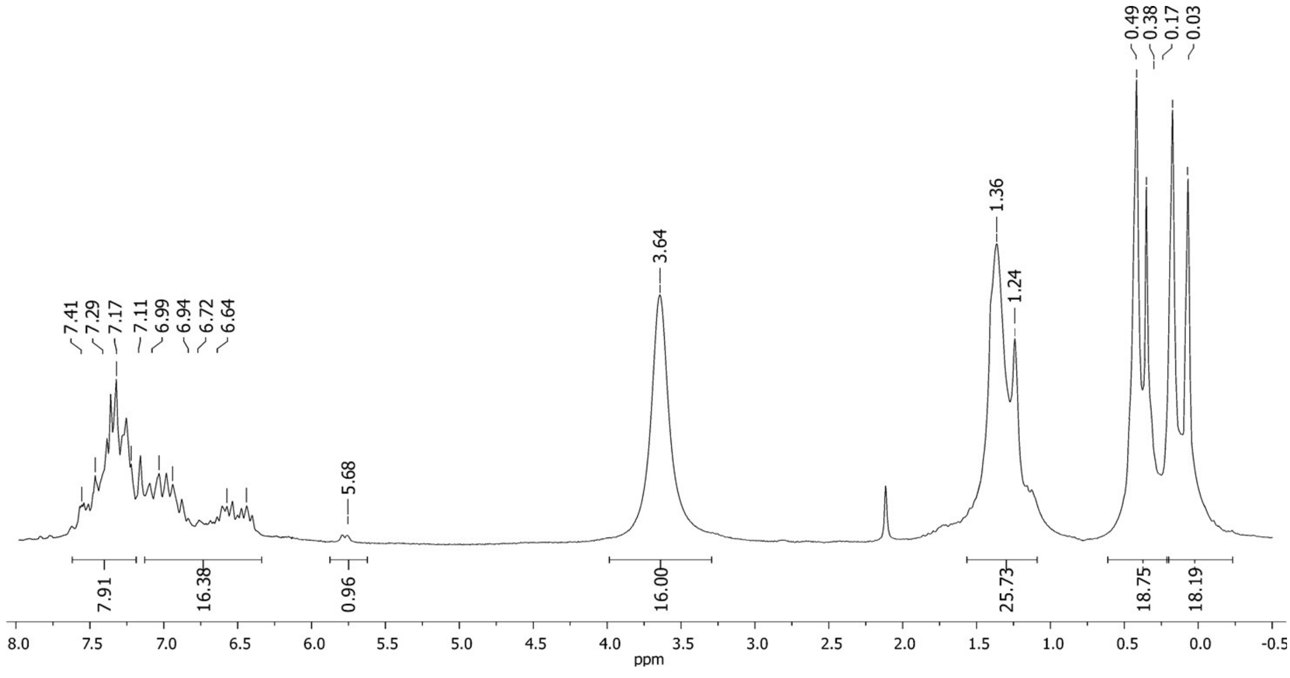

Fig. 18. ^1H NMR spectrum of $[\{1,8\text{-}C_{10}H_6[NSiMe_3][NC(Ph)NSiMe_3]\}\{1,8\text{-}C_{10}H_6[N(H)SiMe_3][NC(Ph)NSiMe_3]\}YOtBu][Li(THF)_4]$ (**7**).

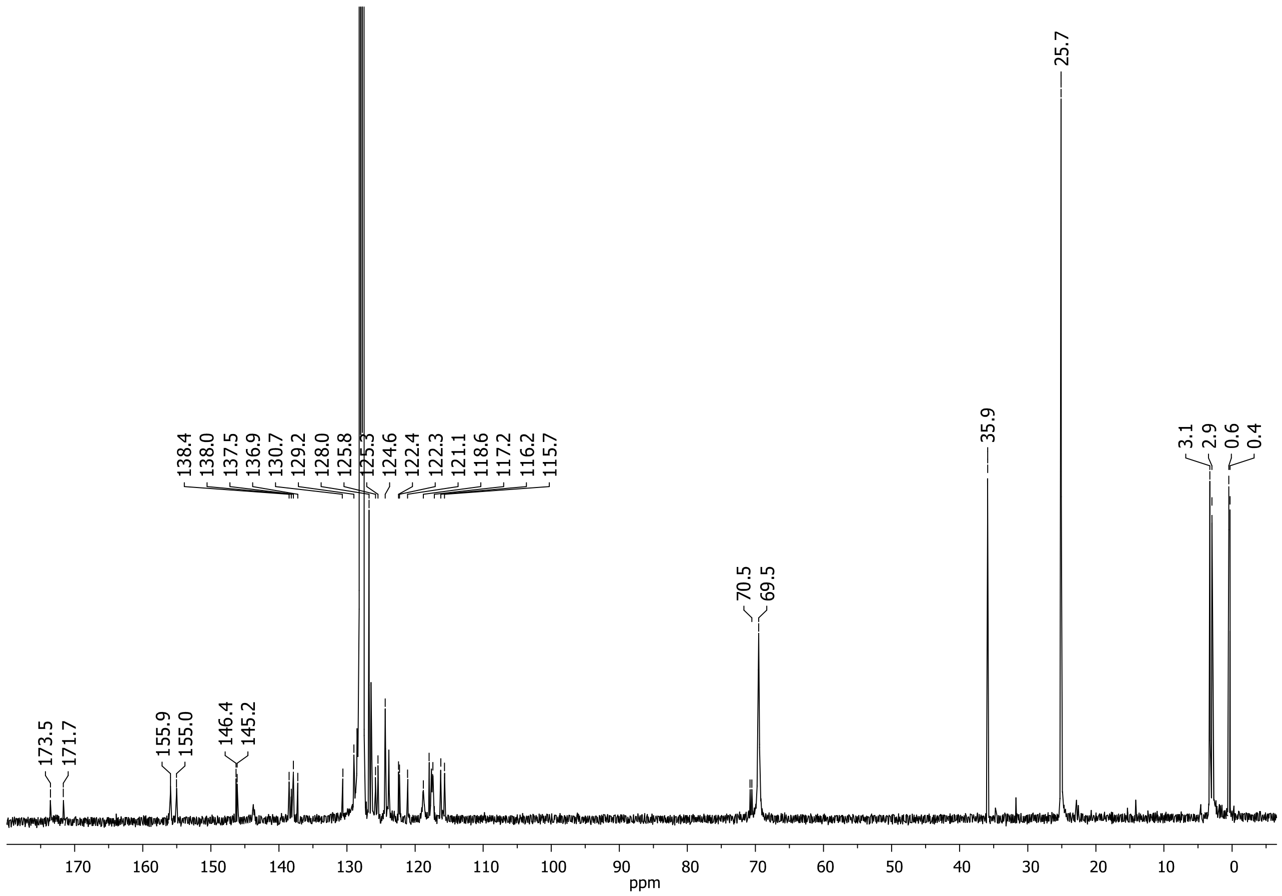

Fig. 19. $^{13}C\{^{1}H\}$ NMR spectrum of [{1,8-$C_{10}H_6$[$NSiMe_3$][NC(Ph)$NSiMe_3$]}{1,8-$C_{10}H_6$[N(H)$SiMe_3$][NC(Ph)$NSiMe_3$]}YOtBu][Li$(THF)_4$] (**7**).

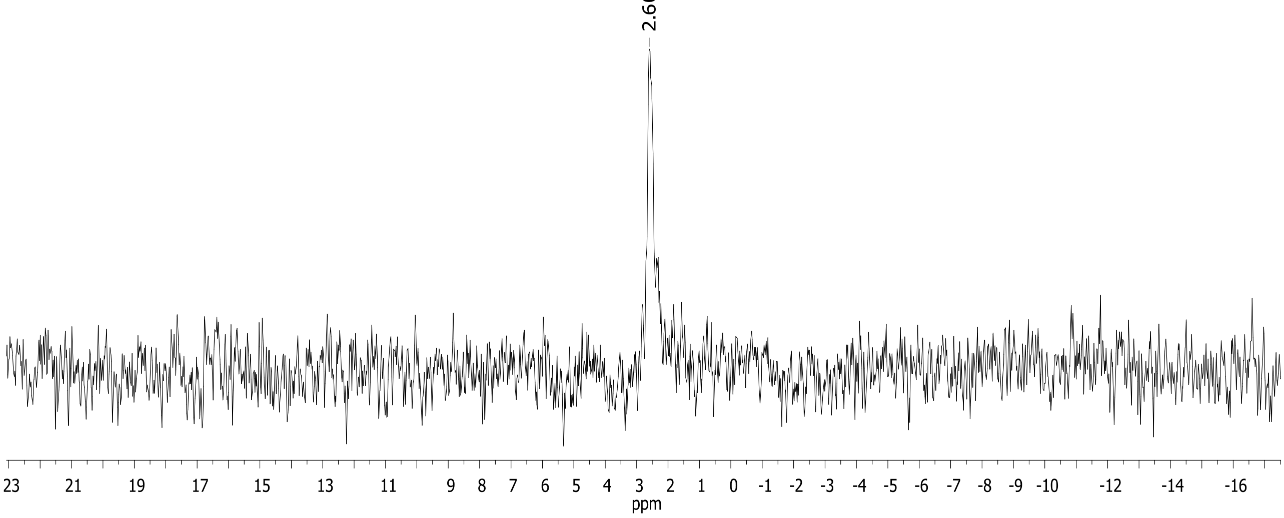

Fig. 20. $^{7}Li\{^{1}H\}$ NMR spectrum of [{1,8-$C_{10}H_6$[$NSiMe_3$][NC(Ph)$NSiMe_3$]}{1,8-$C_{10}H_6$[N(H)$SiMe_3$][NC(Ph)$NSiMe_3$]}YOtBu][Li$(THF)_4$] (**7**).

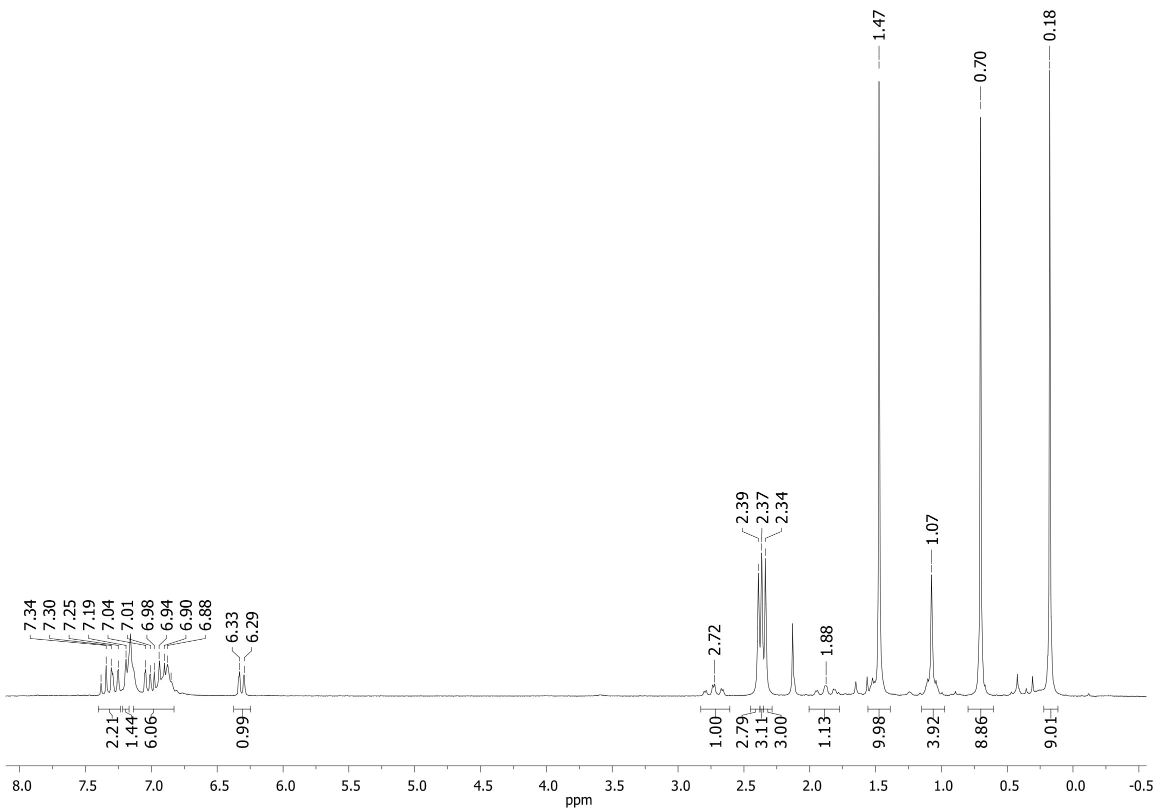

Fig. 21. ^{1}H NMR spectrum of $\{1,8\text{-}C_{10}H_6[NSiMe_3][NC(Ph)NSiMe_3]\}YOtBu(TMEDA)$ (**8**) (400 MHz, C_6D_6, 293 K).

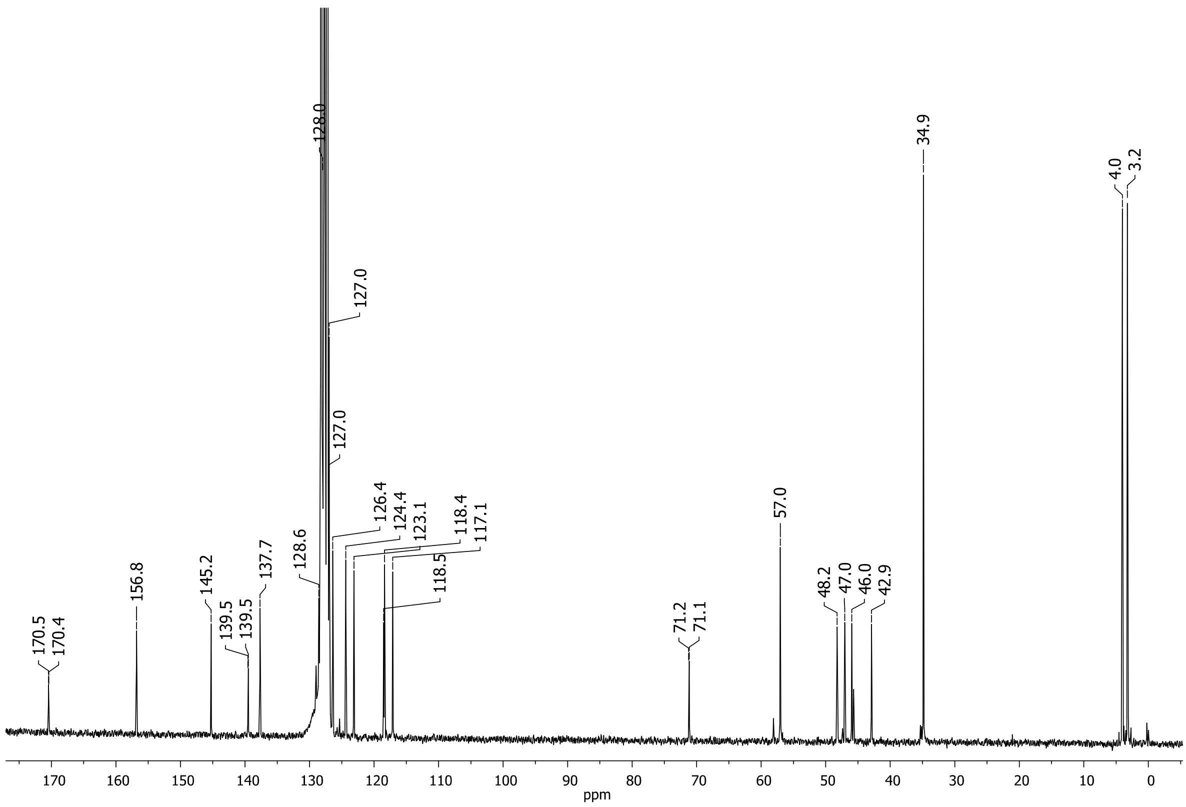

Fig. 22. $^{13}C\{^{1}H\}$ NMR spectrum of $\{1,8\text{-}C_{10}H_6[NSiMe_3][NC(Ph)NSiMe_3]\}YOtBu(TMEDA)$ (**8**) (50 MHz, C_6D_6, 293 K).

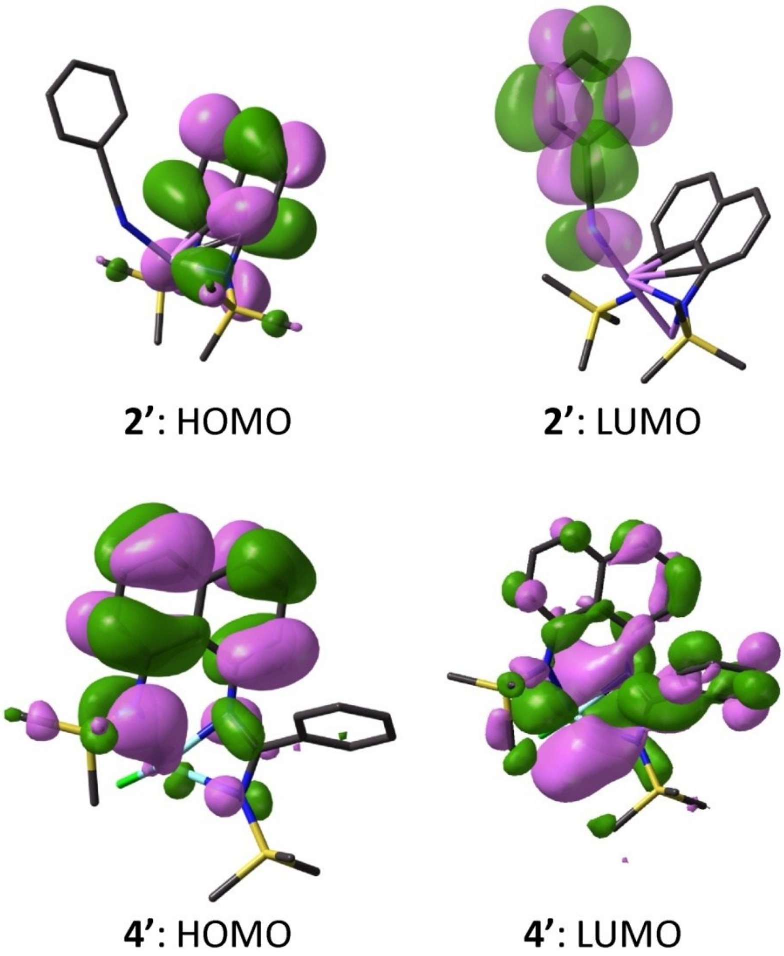

Fig. 23. Isosurfaces (isovalue 0.02) of the frontier molecular orbitals in complexes **2'** (top) and **4'** (bottom)

Full Gaussian 09 reference

Gaussian 09, Revision B.01, M. J. Frisch, G. W. Trucks, H. B. Schlegel, G. E. Scuseria, M. A. Robb, J. R. Cheeseman, G. Scalmani, V. Barone, B. Mennucci, G. A. Petersson, H. Nakatsuji, M. Caricato, X. Li, H. P. Hratchian, A. F. Izmaylov, J. Bloino, G. Zheng, J. L. Sonnenberg, M. Hada, M. Ehara, K. Toyota, R. Fukuda, J. Hasegawa, M. Ishida, T. Nakajima, Y. Honda, O. Kitao, H. Nakai, T. Vreven, J. A. Montgomery, Jr., J. E. Peralta, F. Ogliaro, M. Bearpark, J. J. Heyd, E. Brothers, K. N. Kudin, V. N. Staroverov, R. Kobayashi, J. Normand, K. Raghavachari, A. Rendell, J. C. Burant, S. S. Iyengar, J. Tomasi, M. Cossi, N. Rega, J. M. Millam, M. Klene, J. E. Knox, J. B. Cross, V. Bakken, C. Adamo, J. Jaramillo, R. Gomperts, R. E. Stratmann, O. Yazyev, A. J. Austin, R. Cammi, C. Pomelli, J. W. Ochterski, R. L. Martin, K. Morokuma, V. G. Zakrzewski, G. A. Voth, P. Salvador, J. J. Dannenberg, S. Dapprich, A. D. Daniels, Ö. Farkas, J. B. Foresman, J. V. Ortiz, J. Cioslowski, and D. J. Fox, Gaussian, Inc., Wallingford CT, 2010.

Table S1. Crystal data and structure refinement details for complexes **2^{Et2O}**, **2^{TMEDA}**, **3Y**, **3Sm**, **4**, **7**, **8**.

	2^{Et2O}	**2^{TMEDA}**	**3Y**	**3Sm**	**4**	**7**	**8**
Empirical formula	$C_{31}H_{49}Li_2N_3O_2Si_2$	$C_{29}H_{45}Li_2N_5Si_2{\cdot}(C_7H_8)_{1.5}$	$C_{62}H_{91}ClLiN_6O_4Si_4Y$	$C_{58}H_{89}ClLiN_6O_6Si_4Sm{\cdot}(C_4H_{10}O_2)$	$C_{29}H_{45}ClN_5Si_2Y$	$C_{66}H_{100}LiN_6O_5Si_4Y$	$C_{33}H_{54}N_5OSi_2Y$
FW	565.79	671.96	1228.07	1361.57	644.24	1265.73	681.90
T, K	100(2)	100(2)	100(2)	100(2)	100(2)	150(2)	200(2)
Crystal system	Monoclinic	Monoclinic	Triclinic	Monoclinic	Triclinic	Monoclinic	Monoclinic
Space group	$P2_1/n$	$P2_1/c$	*P-1*	$P2_1/c$	*P-1*	$P2_1/c$	$P2_1/n$
Unit cell dimensions	a [Å] = 10.3401(5) b [Å] = 22.3949(11) c [Å] = 12.6499(7) α [°] = 90 β [°] = 92.4540(10) γ [°] = 90	a [Å] = 10.578(2) b [Å] = 35.496(7) c [Å] = 11.439(2) α [°] = 90 β [°] = 102.82(3) γ [°] = 90	a [Å] = 13.4602(5) b [Å] = 14.5208(5) c [Å] = 17.8410(7) α [°] = 82.8080(10) β [°] = 78.5910(10) γ [°] = 86.2320(10)	a [Å] = 12.4061(4) b [Å] = 27.5182(9) c [Å] = 20.9997(7) α [°] = 90 β [°] = 95.3740(10) γ [°] = 90	a [Å] = 8.7689(6) b [Å] = 11.2424(8) c [Å] = 17.3360(12) α [°] = 87.6876(15) β [°] = 78.3070(15) γ [°] = 76.5725(14)	a [Å] = 13.9163(11) b [Å] = 14.9401(13) c [Å] = 34.281(3) α [°] = 90 β [°] = 97.727(2) γ [°] = 90	a [Å] = 11.4113(7) b [Å] = 27.1287(14) c [Å] = 12.0915(8) α [°] = 90 β [°] = 97.749(5) γ [°] = 90
V, Å^3	3389.3(3)	4188.4(15)	3388.3(2)	7137.6(4)	1627.8(2)	7062.6(10)	3709.0(4)
Z	4	4	2	4	2	2	4
d_{calc}, Mg/m^3	1.109	1.066	1.204	1.267	1.314	1.190	1.221
μ, mm^{-1}	0.134	0.116	1.017	0.979	1.973	0.943	1.668
F(000)	1224	1452	1304	2860	676	2704	1448
Crystal size, mm	0.43×0.38×0.20	0.32×0.15×0.12	0.38×0.26×0.12	0.46×0.16×0.11	0.31×0.20×0.17	0.33×0.21×0.17	0.40×0.25×0.15
θ range for data collection, [°]	2.17–26.00	1.91–27.00	2.12–27.10	1.95–25.04	1.86–27.00	1.77–25.10	3.00–28.70
Index ranges	–12 ≤ h ≤ 12 –27 ≤ k ≤ 27 –18 ≤ l ≤ 17	–13 ≤ h ≤ 13 –42 ≤ k ≤ 45 –14 ≤ l ≤ 12	–17 ≤ h ≤ 17 –18 ≤ k ≤ 18 –22 ≤ l ≤ 22	–14 ≤ h ≤ 14 –32≤ k ≤ 32 –24 ≤ l ≤ 24	–11 ≤ h ≤ 10 –14≤ k ≤ 14 –22≤ l ≤ 22	–16 ≤ h ≤ 14 –16 ≤ k ≤ 17 –35 ≤ l ≤ 40	–10≤ h ≤ 15 –36 ≤ k ≤ 29 –16≤ l ≤16
Reflns collected	28710	25808	31883	56772	14047	38674	21981
Independent reflns (R_{int})	6649 (0.0269)	9145 (0.0373)	14832 (0.0482)	12602 (0.0543)	7039 (0.0304)	12537 (0.1486)	9572 (0.0470)
Completeness to θ	99.8	99.9	99.2	99.9	99.2	99.5	99.9
Data / restraints / parameters	6649 / 0 / 371	9145 / 220 / 512	14832 / 106 / 774	12602 / 612 / 868	7039 / 0 / 353	12537 / 0 / 767	9872 / 123 / 485
GOF on F^2	1.047	1.066	1.016	1.045	1.034	0.953	1.065
Final *R* indices $[I>2\sigma(I)]$	R_1 = 0.0393 wR_2 = 0.0979	R_1 = 0.0680 wR_2 = 0.1462	R_1 = 0.0529 wR_2 = 0.1081	R_1 = 0.0617 wR_2 = 0.1626	R_1 = 0.0376 wR_2 = 0.0822	R_1 = 0.0710 wR_2 = 0.1381	R_1 = 0.0533 wR_2 = 0.0853
R indices (all data)	R_1 = 0.0473 wR_2 = 0.1039	R_1 = 0.0923 wR_2 = 0.1595	R_1 = 0.0937 wR_2 = 0.1239	R_1 = 0.0835 wR_2 = 0.1798	R_1 = 0.0553 wR_2 = 0.886	R_1 = 0.1715 wR_2 = 0.1746	R_1 = 0.0911 wR_2 = 0.0955
Largest diff peak and hole, [e Å^3]	0.38 and –0.20	0.81 and –0.43	0.65 and –0.33	1.81 and –1.04	0.92 and –0.58	0.71 and –0.34	0.39 and −0.41